Phosphorus recovery from pig manure

Elucidating the competition between vivianite and siderite formation

Banke, Sophie; Romero, Jacobo Meca; Monteiro, Alexandre; Prot, Thomas; Korving, Leon; Belloni, Carlo; Schott, Chris; Dugulan, Iulian A.; Loosdrecht, Mark C.M.van

DOI
10.1016/j.cej.2025.169019

Publication date
2025

Document Version
Final published version

Published in
Chemical Engineering Journal

Chemical Engineering Journal 524 (2025) 169019

Contents lists available at ScienceDirect

Chemical Engineering Journal

journal homepage: www.elsevier.com/locate/cej

Phosphorus recovery from pig manure: Elucidating the competition between vivianite and siderite formation

Sophie Banke [a,b,*], Jacobo Meca Romero [a], Alexandre Monteiro [a], Thomas Prot [a], Leon Korving [a], Carlo Belloni [a], Chris Schott [a], Iulian A. Dugulan [c], Mark C. M.van Loosdrecht [b]

[a] Wetsus, European Centre of Excellence for Sustainable Water Technology, Oostergoweg 9, 8911 MA, Leeuwarden, the Netherlands
[b] Department of Biotechnology, Delft University of Technology, Van der Maasweg 9, Delft, 2629 HZ, the Netherlands
[c] Department of Radiation Science and Technology, Delft University of Technology, Mekelweg 15, Delft, 2629 JB, the Netherlands

ARTICLE INFO

Keywords:
Dissolved inorganic carbon
Alkalinity
Anaerobic digestion
Thermal hydrolysis plant sludge
ammonia stripping
Integrated resource recovery
Nutrient recovery

ABSTRACT

Phosphorus runoff from agricultural land is a major driver of eutrophication, with manure serving as a significant source of phosphorus input. In regions such as the Netherlands, high livestock densities and limited land availability pose challenges for manure management, particularly in pig farming. Recovering phosphorus from manure and redistributing it to phosphorus-deficient areas offers a sustainable solution. This study explores phosphate recovery via vivianite ($Fe_3(PO_4)_2{\cdot}8H_2O$) precipitation—a method previously demonstrated in municipal wastewater treatment plant sludge—and evaluates its applicability to pig manure. Vivianite formation was investigated in fresh, 4-month-aged, and digested pig manure, as well as in Thermal Hydrolysis Plant (THP) derived digested sewage sludge. A key finding is that high dissolved inorganic carbon (DIC) concentrations inhibit vivianite formation by promoting siderite ($FeCO_3$) precipitation. In digested manure, a DIC threshold of approximately 3 g/L HCO_3^- was identified, below which vivianite formation is favored. THP sludge, characterized by elevated DIC, exhibited similar inhibitory effects. More generally, vivianite was shown to form without significant competition with siderite if the DIC concentration is <2.5 times the iron concentration. Experimental results were compared with thermodynamic predictions using Visual MINTEQ and experiments in ultrapure water, revealing discrepancies which may be attributed to the ionic composition in environmental matrices. Strategies such as combining ammonia and DIC stripping or targeting fresh manure were shown to enhance vivianite formation. These findings can be used to propose the integration of vivianite-based phosphorus recovery into broader resource recovery frameworks, including biomethane production, ammonium recovery, and carbon capture.

1. Introduction

Phosphate fertilizers play a critical role in modern agriculture, with a substantial portion of phosphate input in European soils originating from manure application [1,2]. However, manure-based phosphorus (P) is often applied in excess, leading to runoff into surrounding water bodies. This runoff accelerates eutrophication, resulting in algal blooms and hypoxic conditions that threaten aquatic ecosystems, where phosphate is frequently the limiting nutrient [3,4]. Elevated phosphate concentrations are particularly prevalent in regions with intensive agricultural activity, such as the Netherlands, Belgium, Denmark, and northwestern Germany [1,2]. Regulatory restrictions on manure spreading in areas like the Netherlands have led to the export of surplus manure, which incurs additional costs and results in the loss of valuable organic matter [5,6].

To address this issue, phosphate recovery from manure and its reutilization as a secondary resource in phosphate-based industries has been proposed [7]. In manure, phosphorus predominantly exists as magnesium ammonium phosphate (struvite) and calcium phosphates, typically in particulate forms smaller than 150 μm in both cattle and pig manure [8,9]. Especially in the Netherlands, pig farmers are challenged by the high livestock density in pig farming and the increased amount of

* Corresponding author at: Wetsus, European Centre of Excellence for Sustainable Water Technology, Oostergoweg 9, 8911 MA, Leeuwarden, the Netherlands.
E-mail addresses: sbanke@tudelft.nl (S. Banke), jacobo.meca@wetsus.nl (J.M. Romero), alexandre.monteiro@wetsus.nl (A. Monteiro), thomas.prot@wetsus.nl (T. Prot), leon.korving@wetsus.nl (L. Korving), carlo.belloni@wetsus.nl (C. Belloni), chris.schott@wetsus.nl (C. Schott), a.i.dugulan@tudelft.nl (I.A. Dugulan), M.C.M.vanLoosdrecht@tudelft.nl (M.C.M.van Loosdrecht).

https://doi.org/10.1016/j.cej.2025.169019
Received 22 July 2025; Received in revised form 11 September 2025; Accepted 26 September 2025
Available online 29 September 2025

land necessary to dispose of the manure [10]. This intensification makes pig manure a particularly suitable target for nutrient recovery technologies, which could enable the redistribution of phosphorus from regions with surplus to those with a deficit. Commonly employed manure treatment methods include composting and solid-liquid separation followed by pelleting. However, due to the typically low nitrogen-to-phosphorus (N/P) ratio and high transportation costs, physical treatment alone is often insufficient to address nutrient imbalances and environmental concerns [11]. In recent years, thermochemical conversion technologies such as pyrolysis and hydrothermal carbonization have gained attention for their ability to mitigate odor, reduce greenhouse gas emissions, and eliminate pathogens, while simultaneously lowering the risk of water and soil contamination [11,12]. Despite these benefits, the resulting biochar and hydrochar exhibit considerable heterogeneity in elemental composition and phosphorus speciation [13], which complicates their direct use to make phosphorus-based products. Targeted phosphorus recovery from these materials often necessitates additional chemical extraction steps. In contrast, precipitation-based approaches—such as the formation of struvite or calcium phosphate—enable the recovery of phosphorus in a more defined mineral phase, offering a more controlled and efficient pathway for nutrient recycling [11]. Current precipitation techniques often involve acidification followed by reprecipitation with alkaline salts, a process that entails substantial chemical consumption [7,14,15]. A promising alternative lies in transforming these phosphorus precipitates into a single mineral phase—vivianite ($Fe(II)_3(PO_4)_2{\cdot}8H_2O$)—through iron dosing. Vivianite, a paramagnetic iron (Fe) phosphate mineral, is known to form under anaerobic conditions and has been successfully recovered magnetically at pilot scale from sewage sludge digesters [16–18]. Its thermodynamic stability within pH 6–8 [19] renders it a potentially favorable sink for phosphate, offering a recovery method that circumvents the need for heavy acidification and reprecipitation.

Initial proof-of-principle experiments demonstrated that vivianite indeed forms in pig manure at laboratory scale, with most phosphate recovered at a Fe/P molar ratio of 4.5 [20]. This is considerably higher than the optimal Fe/P ratio of 1.6–1.9 reported for sewage sludge, which is itself only slightly above the theoretical stoichiometric ratio of 1.5. The need for elevated iron dosing in manure not only increases chemical costs but also leaves behind iron-rich residues that may limit the agronomic value of the treated manure [21]. The underlying cause of this inefficiency remains unclear, necessitating further investigation into iron interactions within manure. Sulfide has been identified as a thermodynamically favored competitor for iron binding over phosphate [22], but sulfur content alone does not fully account for the high iron requirements observed. Insights from sediment studies suggest that organic matter may sequester iron, potentially limiting its availability for vivianite formation [23,24]. However, recent findings indicate that dissolved organic matter in manure does not bind iron strongly enough to impede vivianite precipitation [25]. Given that neither sulfide precipitation nor organic complexation fully explains the observed inefficiency in vivianite formation, additional factors must be considered. Thermodynamic modeling in this study indicates that under elevated levels of dissolved inorganic carbon (DIC), the formation of ferrous carbonate (siderite) is thermodynamically favored, potentially outcompeting vivianite precipitation. While the influence of DIC on struvite and calcium phosphate formation has been previously explored [26–28], its role in the competition between siderite and vivianite in manure systems has not yet been addressed.

In this study, DIC is used to describe carbonate chemistry relevant to mineral precipitation. However, DIC is closely related to alkalinity, a parameter more commonly used in agricultural contexts. Under the near-neutral pH conditions typical of manure and sludge, alkalinity is primarily governed by bicarbonate (HCO_3^-), the dominant DIC species. Therefore, DIC serves as a chemically precise proxy for alkalinity in this context. This work investigates the impact of DIC on vivianite formation across manure matrices with varying DIC concentrations and proposes mitigation strategies to enhance phosphate recovery, including DIC stripping and targeting low-DIC substrates.

2. Material & methods

2.1. Pig manure preparation and characteristics

Fresh pig manure was collected in September 2023 from the Tijs farm located in Hoge Hexel, the Netherlands (3900 feeder pigs with straw bedding). The experiment with fresh manure was conducted shortly after collection. To simulate manure aging under controlled conditions, fresh manure was stored in a jerry can equipped with a gas exhaust system at ambient laboratory temperature (23 °C) for a period of four months. Notice that, in the Netherlands, approximately 30 % of manure was stored in pits as of 2020, with the remainder managed through systems such as solid-liquid separation or deep litter bedding [29]. On Dutch pig farms, manure was typically retained in storage pits for durations ranging from six months to one year [30]. Given that ambient outdoor temperatures in the Netherlands are generally lower than laboratory conditions, the elevated temperature during laboratory storage may partially compensate for the shorter retention time. Consequently, this setup approximates the partial anaerobic digestion that occurs during pit storage, albeit under more controlled and accelerated conditions. In addition, mono-digested manure from the same source, collected at the same time, was used in a separate set of experiments conducted in May 2024. The digester temperature was 38 °C with a retention time of 40 days [31]. The composition of these three manure types—fresh, 4-month-aged, and digested—is summarized in Table 1.

2.1.1. Stripping digested manure

Unlike fresh and aged manure, digested manure can contain a more heterogeneous mixture of feedstocks [32] and is often supplemented with additives, such as iron salts (Table 2), to suppress hydrogen sulfide emissions [33]. Despite this complexity, digested manure offers operational advantages for phosphorus recovery, including lower solids content and wider adoption of anaerobic digestion for biogas production [34]. Integrating vivianite-based phosphate recovery into existing digestion infrastructure presents a promising pathway for circularity.

To enhance vivianite formation and minimize excessive iron dosing, DIC was removed from digested manure via gas stripping (Fig. A 1). This process involved purging 1.5 L of digested manure in a 5 L bottle with nitrogen gas under continuous magnetic stirring (Heidolph), while collecting the stripped CO_2 in a 0.1 M NaOH solution. This method

Table 1
Total elements of microwave-digested and soluble fraction of 0.45 µm filtered fresh, 4-month-aged, and digested manure.

c (g/kg dried)	Fresh manure	4-month-aged manure	Digested manure
	total elements (N = 3)		
Mg	20 ± 1	16 ± 2	26 ± 1
P	18 ± 1	14 ± 2	30 ± 1
Fe	1.9 ± 0.2	1.4 ± 0.2	18 ± 1
S	14 ± 1	11 ± 2	23 ± 1
Ca	29 ± 2	26 ± 5	41 ± 1
TS (g/kg)	123 ± 1	132 ± 2	55 ± 1
VS (g/kg)	98 ± 1	101 ± 2	35 ± 1
mg/L	soluble fraction (*N* = 3)		
Mg	570 ± 20	352 ± 4	30 ± 1
P	7.9 ± 0.3	11.9 ± 0.4	17 ± 1
Fe	–	–	22 ± 1
S	540 ± 20	540 ± 80	112 ± 1
Ca	290 ± 30	61 ± 2	12.6 ± 0.5
K^+	5550 ± 40	6140 ± 40	5510 ± 80
Na^+	1770 ± 50	1910 ± 50	1610 ± 90
Cl^-	3580 (*N* = 1)	3650 ± 40	2730 ± 40
NH_4^+	7040 (N = 1)	7220 ± 40	7530 ± 30
HCO_3^-	6700 (N = 1)	19,500 (N = 1)	23,000 ± 2000
pH	7.0	7.7	8.7

Table 2
Iron dosing experiments in different manure, with manure volume, batch type, iron dose added to the manure, and soluble phase sampling points.

	V (L)	Batch type	Fe added (g/L)	soluble phase sampling times (h) (for ICP)
Fresh	0.5	Triplicate with blank	7.9	1, 2, 3.5, 6, 24*^, 48^, 168^, 336^, and 504*^ h
4-month-aged	0.5	triplicate with blank	6.8	1, 6^, 24*^, 48^, 192^, and 384*^ h
Stripped digested	0.2	0, 24, 48, 96, 168 h stripped	5.6	1, 4, 24, and 48 h

*sampling points include $NH4^+$, ^sampling points include DIC.

facilitates the combined removal of ammonia and CO_2 without using a base to increase the pH (for ammonia stripping), or an acid (for CO_2 stripping) (Eqs. (1) and (2)). Overall, the pH increased during the process, implying that the protonation of DIC cost more protons than the deprotonation of ammonium (Fig. A 1).

$$HCO_3^- (aq) \xrightarrow{\text{Stripping gas}} OH^- (aq) + CO_2 (g) \quad (1)$$

$$NH_4^+ (aq) + OH^- (aq) \xrightarrow{\text{Stripping gas}} NH_3 (g) + H_2O (l) \quad (2)$$

Samples (200 mL + 5 mL for analysis) were collected after 0 h, 24 h, 48 h, 96 h, and 168 h of stripping. As CO_2 removal increased the pH, samples were acidified to pH 8 using 2 M HCl (Titrando) to optimize conditions for vivianite formation [19], with the resulting DIC concentrations ranging from 30 mM to 220 mM.

2.2. Iron dosing experiments

2.2.1. In fresh, 4-month-aged, and digested manure

To investigate the prevalence of struvite, vivianite, and siderite under varying concentrations of dissolved inorganic carbon (DIC), a series of iron dosing experiments were conducted using three distinct manure matrices: fresh manure, 4-month-aged manure, and stripped digested manure. Iron(II) chloride tetrahydrate ($FeCl_2{\cdot}4H_2O$) from a 10.7 M stock solution was introduced in the manure, first at a stoichiometric Fe/S molar ratio of 1 to facilitate sulfur binding, and then at a Fe/P ratio of 1.5 to promote vivianite formation. Iron addition was performed gradually with intermittent stirring to mitigate foam formation resulting from gas release. All treatments were conducted in triplicate, alongside control samples without iron addition. The experimental vessels were sealed, connected to a gas exhaust system, and incubated at room temperature on a rotary platform shaker (Heidolph Unimax 2010) operating at 100 rpm for a duration of up to two weeks. Sampling (5 mL per time point) was performed at regular intervals to monitor soluble elements, ammonium, and DIC concentrations. By monitoring the soluble phase, dissolution and precipitation processes can be tracked, inferring information on phase transformation in the solid phase. Since the experiments on the different manure types were performed sequentially, the sampling times were readjusted for each experiment. The soluble phase did not change much after 48 h in the fresh manure experiment, which was executed first. Therefore, the 4-month-aged experiment was terminated after 384 h, and after 48 h for digested manure, the latter reflecting a more practical timeframe for applied settings. The complete overview of experimental volumes and sampling time points is provided in Table 2. At the final sampling point, 50 mL were withdrawn from each bottle for solids analysis to determine the different mineral phases in the sample and quantify the amount of vivianite and siderite.

2.2.2. In ultrapure water

To isolate the role of DIC without the complexity of manure matrices, additional experiments on vivianite formation were conducted in ultrapure water. Struvite ($MgNH_4PO_4{*}6\ H_2O$) from the water authority Aa & Maas in the Netherlands (via Aquaminerals) was used as phosphorus feedstock. In a glovebox (DO<0.1 %), $NaHCO_3$ was added at different DIC concentrations (3, 30, and 300 mM) to 100 mL serum bottles containing struvite (5 mM of P), and the pH was adjusted to 8 (Table A 1). Iron was added from the 10.7 M $FeCl_2{\cdot}4H_2O$ stock solution at a stoichiometric Fe/P ratio of 1.5 (7.5 mM Fe). The ultrapure system used 10-fold lower concentrations of both struvite and iron compared to the manure experiments, in order to limit pH shifts in a system with limited buffering capacity. Therefore, the struvite-to-DIC ratios in the 3 and 30 mM DIC experiments were comparable to those in fresh and aged manure, respectively. The bottles were shaken at room temperature at 100 rpm for two weeks. Aliquots (1.5 mL) were collected at 0.5 h, 1.5 h, 3.5 h, 6 h, 24 h, 48 h, 168 h, and 336 h for analysis.

2.3. Characterization

For soluble phase analysis, samples were centrifuged at 4750 rpm for 10 min (Beckman Coulter, Avanti J-15R), and the supernatant was filtered through 0.45 μm syringe filters (Millipore). Elemental concentrations were measured by Inductively Coupled Plasma Optical Emission Spectroscopy (ICP-OES; Thermo Scientific iCAP Pro, with yttrium standard). Ammonium was quantified using ion chromatography (Metrohm Compact IC Flex 88), and DIC was determined via total organic carbon analysis (TOC-L CPH, Shimadzu) [27,28].

Manure total elemental composition was assessed via microwave digestion of 2 mL wet samples in 69 % HNO_3 using a sludge and solids protocol (180 °C for 15 min) (Milestone Ethos Easy) [27,28], followed by ICP-OES analysis.

For solid phase analysis, the final samples (50 mL) were centrifuged at 4750 rpm for 10 min and imported into a glovebox with N_2 atmosphere (25 °C). The supernatant was decanted inside the glovebox, the solids were spread out in petri dishes, and dried under an aluminum cover with small holes for aeration to minimize light exposure of the samples. Characterization included the following:

- Scanning Electron Microscopy (SEM; JEOL JSM-6480LV) coupled with Energy Dispersive X-ray Spectroscopy (EDX; Oxford Instruments x-act SDD Energy Dispersive X-ray spectrometer) to investigate morphology and elemental distribution [35,36]. Small pieces of the dried manure were stuck on the SEM-EDX holder in the glovebox, but air-exposed when mounting the samples in the apparatus. Samples were then gold-coated (10 nm) under vacuum (15 Pa, 25 mA), and measurements were taken at 12 kV with a 10 mm working distance. Data acquisition and analysis were performed using JEOL and Aztec software.
- X-Ray Diffraction (XRD; PBruker D8 Advance diffractometer), to investigate crystalline phases as previously done on digested sludge [35], was performed on samples ground in the glovebox, and sent for measurement in parafilm-sealed tubes, but air-exposed during analysis. Powders were mounted on Si510 wafers, scanned with Cu Kα radiation (5°–80° 2θ, 0.008° step size, 2 s/step), and analyzed using Bruker DiffracSuite EVA software.
- Mössbauer Spectroscopy, to speciate and quantify iron phases as has previously been established for digested sludge samples [35,37,38]. Measurements were performed at 295 K, with conventional constant acceleration or sinusoidal velocity spectrometer, using a $^{57}Co(Rh)$ radioactive with a α-Fe as calibration reference. Samples were ground and sealed in the glovebox before exporting them outside for measurements. For the 4-month-aged manure, additional measurements were conducted at 4 K due to unclear vivianite signals at room temperature. At this temperature, magnetic ordering permits more definitive phase identification due to sextet formation [39]. Spectra were analyzed using MossWinn 4.0 [40].

The phosphate fraction bound to the iron in vivianite detected with Mössbauer Spectroscopy was estimated using Eq. (3):

$$\% \text{ P vivianite} = \frac{(\% \text{ Fe vivianite A} + \% \text{ Fe vivianite B}) \bullet \text{total Fe}}{1.5 \bullet \text{total P}} \bullet 100\% \quad (3)$$

With % Fe vivianite A and B as determined by Mössbauer spectroscopy, total Fe and P, the total molar concentration of the element determined at the end of the experiment, and the factor 1.5 reflects the molar Fe/P ratio typical of stoichiometric vivianite. The error on this value was calculated using Gaussian error propagation and assuming an error of 3 % on total elemental concentrations based on the error margins in Table 1.

2.4. MINTEQ calculations

Visual MINTEQ was used to simulate how vivianite precipitation in fresh, 4-month-aged, and stripped digested manure is affected by varying DIC and NH_4^+ concentrations. Model inputs were based on measured elemental compositions (Table 1) and ion chromatography results for Na^+, Cl^-, and K^+. DIC and NH_4^+ concentrations could only be measured in the liquid phase. However, XRD indicated the presence of these ions to also be present in the solid phase, as calcite and struvite respectively (Fig. 2). Hence, the input for CO_3^{2-} was the sum of DIC and the equimolar concentration of total calcium assuming most calcium was bound in calcite, and the input for NH_4^+ was the sum of soluble NH_4^+ and the equimolar concentration of total phosphorus assuming most phosphorus was bound as struvite. For HS^- total sulfur was input assuming most sulfur to be present as sulfide in the anaerobic conditions of the manures (Section 3.1). Simulations were conducted at the final pH of each experiment, using the Specific Ion Interaction Theory (SIT) modeling [41], with details provided in Table 3.

3. Results & discussion

3.1. Vivianite vs siderite formation in manure

The presence of phosphate in fresh and 4-month-aged manure with and without iron addition was studied by SEM-EDX analysis (Fig. 1). Elemental mapping revealed a predominant co-localization of magnesium and phosphorus in the blank manures, suggesting that magnesium-bound phosphorus is the dominant P species in both fresh and 4-month-aged manures. The morphology of these phosphorus-rich regions, characterized by well-defined, box-like structures, is consistent with struvite ($MgNH_4PO_4{\cdot}6H_2O$) crystals [72]. This interpretation was corroborated by X-ray diffraction (XRD) data (Fig. 2), which confirmed the presence of struvite and showed the presence of calcite in the blank samples. A notable feature in the XRD patterns is the broad hump with the struvite peak at approximately 20° 2θ, suggesting potential structural disorder in struvite, or the presence of poorly crystalline or ultrafine particles. Most of the phosphorus is likely present as struvite. Based on the elemental composition of the manures (Table 1), there is enough magnesium to bind all the phosphate in struvite (struvite Mg/P = 1). Nevertheless, the presence of calcium phosphate is not uncommon in manure [42] and a small amount of the phosphate could be bound to calcium in this manure, since SEM-EDX imaging revealed a few particles in fresh manure where calcium and phosphorus signals overlapped.

Upon iron addition, the iron precipitated in both fresh and 4-month-aged manure, with a quicker precipitation in the latter (Fig. A 2). Moreover, the DIC decreased in both manures, with a bigger decrease for the 4-month-aged manure. In the fresh manure, roughly 80 % of the magnesium was released into the solution within 24 h, indicating the dissolution of struvite (Fig. A 2). The pH dropped from 7.0 to 6.8 in the fresh manure and 7.7 to 7.2 in the 4-month-aged manure over the course of the experiment. The SEM-EDX analysis of the solids shows a co-localization of iron and phosphorus elemental maps in the fresh manure. The iron and phosphorus maps are congruent with round shapes approximately 10–20 μm in diameter, indicating vivianite. In the 4-month-old manure, the predominant magnesium and phosphorus co-localization was observed, as in the blank manures, indicating struvite. The iron distribution in this sample appeared more diffuse, with a reduction in high-density agglomerates that would indicate mineral formation. XRD patterns revealed the disappearance of struvite reflexes in fresh manure, with new peaks appearing, corresponding to vivianite ($Fe_3(PO_4)_2{\cdot}8H_2O$). Moreover, reflexes that are likely attributed to KCl are more intense in this sample, which could be related to the sample containing more liquid before it started drying. Both K^+ and Cl^- concentrations are high in the liquid phase of the manure and are deposited during the manure drying process. In contrast to the fresh manure, the 4-month manure retained some struvite and calcite but also exhibited weaker vivianite signals. Notably, an additional crystalline phase corresponding to siderite ($FeCO_3$) emerged in the 4-month-aged manure.

The Mössbauer spectroscopy analysis, presented in Fig. 3 and Table 4, further elucidated the nature of iron speciation in Fe-dosed fresh and 4-month-aged manures. For both manures, vivianite was identified at 295 K by the presence of two distinct doublets representing the two unique Fe(II) environments within the vivianite structure with one iron atom in site A and two iron atoms in site B per unit cell [43]. These doublets can be identified as vivianite with isomer shifts (IS) of 1.16 and 1.20, and quadrupole shifts (QS) of 2.45 and 2.91 in the literature [44]. In fresh manure, the Mössbauer fitting suggests that 64 % of the total iron was present as vivianite. Based on Eq. 3, this would account for 97 ± 6 % of the total phosphorus. The remaining 36 % of iron was attributed to either Fe(III) (such as oxidized vivianite [37] species or low-spin Fe(II), possibly arising from iron sulfides. Given that most phosphate would be bound in vivianite based on the Fe (II) vivianite A and B contributions alone, and that iron sulfides are thermodynamically favored under reducing conditions [22], this portion of the iron is likely present as an iron sulfide phase, in agreement with previous studies [45]. Moreover, studies on digested sludge assumed the stoichiometry of Fe/S to be 1 [35] which is a typical stoichiometry of iron sulfide phases [46]. The calculations of the percentage of iron bound to sulfur based on this stoichiometric ratio and the measured elemental composition of manure, the sulfur concentration would account for 37 % of the total iron, consistent with the Mössbauer-derived value of 36 %.

Vivianite could also be observed in 4-month-aged manure. While the parameters are well aligned with literature [44], the distribution between the two vivianite sites A and B is not according to the stoichiometric ratio. Theoretically, site B should have double the contribution of site A, since two iron atoms are in site B and one is in site A as defined for the vivianite crystal structure. However, here, the site A contribution is 1.5 times higher than site B. Partial substitution of iron by magnesium could explain this distortion [47], but could not be proven with SEM-

Table 3
Input values for MINTEQ calculations based on the SIT ionic activity model, with varying DIC and ammonium values. List of possible solids: $Ca_3(PO_4)_2$ (am2), $CaHPO_4{:}2H_2O$(s), Mackinawite, Vivianite, Struvite, Siderite, $MgHPO_4{:}3H_2O$(s), Calcite, Magnesite, $Fe(OH)_2$ (am).

	c (mM)						
			Digested manure				
Component	Fresh	4-month-aged manure	30 mM DIC	55 mM DIC	75 mM DIC	135 mM DIC	220 mM DIC
CO_3^{2-}	200	410	90	115	135	195	280
NH_4^+	460	460	50	100	200	345	430
Fe^{2+}	140	120	135	120	115	115	115
PO_4^{3-}	70	60	80	70	60	50	55
HS^-	55	45	55	50	40	35	40
Ca^{2+}	90	90	120	75	70	60	60
Mg^{2+}	100	90	85	75	65	55	55
K^+	140	155	140	140	140	140	140
Na^+	75	80	70	70	70	70	70
Cl^-	200	200	290	290	290	290	290
pH	7.0	7.5	7.1	7.3	7.6	7.6	7.9

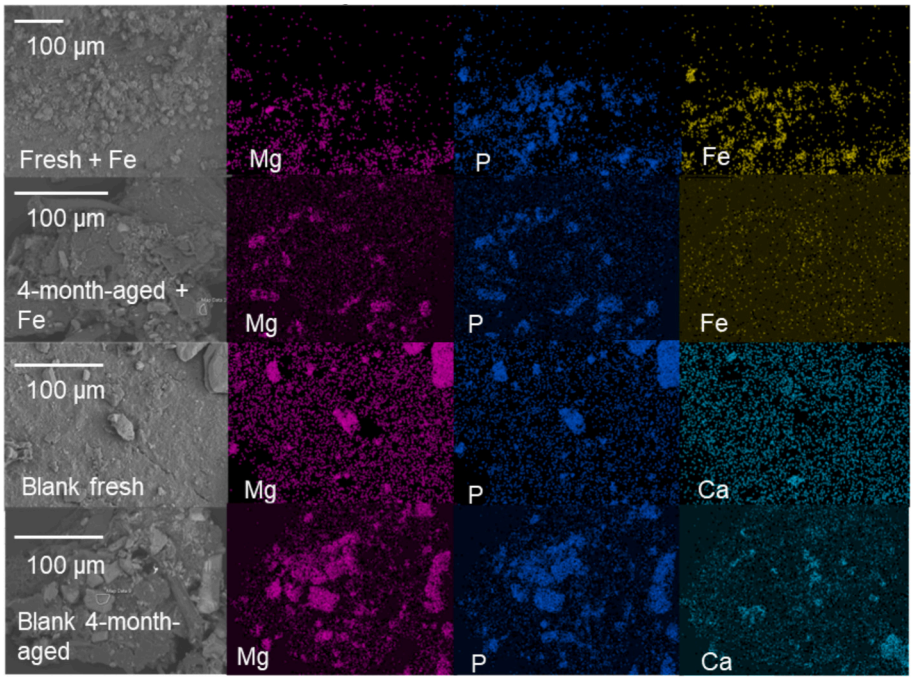

Fig. 1. Electron microscopy images of iron-dosed fresh manure and 4-month-aged manure, as well as respective blanks. The EDX maps of Mg, Ca, Fe, and P highlight the presence of phosphate as vivianite in the iron-dosed fresh manure, and as struvite in the others.

EDX (Fig. A 3). A preferred oxidation at site B could explain the smaller contribution of this site in 4-month-aged manure better. Counting only iron(II) vivianite contributions 49 % of the phosphate would be bound as vivianite. To improve iron phase discrimination, low-temperature (4 K) Mössbauer measurements were conducted. However, the complexity of the spectrum increased, likely due to fine particle size and compositional heterogeneity [48]. At 4 K the two fully split sextuplets of vivianite can be identified, indicating that 27 % of total iron was in vivianite, translating to ~41 % of the phosphate present. In this case, the site ratio A/B was one, still indicating a reduced contribution of site B as observed at 295 K. Oxidation of the vivianite remains a likely explanation for this, with Fe (III) contributions clearly distinguishable in the 4 K spectrum (light and dark brown lines for oxidation in site A and B respectively in Fig. 3). Adding Fe(II) and Fe(III) components, the total amount of iron would be 22 % in site A and 29 % in site B. Even then, the B/A ratio is only 1.3, so impurities such as magnesium remain an option even though SEM-EDX might not have been sensitive enough to detect them.

A substantial difference between the fresh and 4-month-aged manure iron speciation is the siderite present in 4-month-aged manure, accounting for approximately 36 % of the total iron content, as determined by Mössbauer spectroscopy. The isomer shift and quadrupole splitting closely match the characteristic values reported for siderite (IS = 1.22, QS = 1.80) [49] confirming its presence. The competitive formation of siderite and vivianite has been documented in both natural and engineered environments. For instance, Chen et al. (2022) observed reduced phosphate precipitation in the presence of equimolar concentrations DIC and phosphate in synthetic kitchen waste, suggesting that DIC can compete with phosphate and thus inhibit vivianite formation [50]. The presence of siderite in the same place as vivianite has also been reported in lake sediments and has been related to pH, with vivianite prevailing at pH 6 and siderite at pH 8 [51]. However, the nature of the composition in iron-dosed manure is very different from lake sediments, with magnitudes higher concentrations of iron, phosphate, and carbonate. In the present study, the pH was 7.0 in fresh manure and 7.2 in 4-month-aged manure at the end of the experiment, which is a minor difference compared to the concentrations of theses ions, and therefore unlikely to be the dominant factor influencing the iron phase formation. Instead, the markedly higher DIC concentration in the aged manure—approximately 320 mM (20 g/L HCO_3^-) compared to 110 mM (7 g/L HCO_3^-) in the fresh manure—likely shifted the chemical equilibrium toward siderite precipitation. Similar observations were made for calcium phosphate granulation in cow manure [27]; and struvite formation in dairy manure [52] where a high DIC precipitated the calcium and magnesium cations instead of phosphate. With the experiments here, it is shown that the inhibitory effect of DIC in manure also extends to ferrous phosphate formation.

3.2. *Vivianite vs siderite formation in ultrapure water*

To reproduce the influence of DIC on struvite dissolution and vivianite formation, precipitation in ultrapure water with increasing DIC concentrations (3, 30, 300 mM) was evaluated. The temporal evolutions of iron, magnesium, phosphorus, and DIC in the liquid phase are presented in Fig. 4. The results indicate that increasing DIC concentrations accelerate iron precipitation in the form of siderite. Concurrently, magnesium and phosphorus—initially present as struvite—were released into solution as struvite dissolved. Notably, higher DIC concentrations led to a more pronounced release of both ions. This observation is in contrast with the results from iron dosing in 4-month-aged manure, where elevated DIC did not result in significant phosphorus and magnesium release. The DIC of the 30 mM sample displayed an interesting pattern, with the DIC decreasing at the beginning only to increase again after 24 h. This suggests that first DIC precipitated as siderite and then redissolved. The pH decreased in the 3 and 30 mM experiments from 7.7 to 7.3 and 7.8 to 7.5, respectively, and slightly increased in the 0 and 300 mM samples from 7.5 to 7.6 and 7.9 to 8.1, respectively. A decrease in pH could be due to the addition of $FeCl_2$, an acidic salt, and due to the deprotonation of bicarbonate during siderite formation. Struvite dissolution, however, increases the pH due to the release of deprotonated phosphate. Vivianite formation should not change the pH much since the deprotonated phosphate would be incorporated into the vivianite structure. It seems struvite dissolution is the dominant factor influencing the pH in the 0 and 300 mM samples, while siderite precipitation seems to mainly influence the pH in the 3 and 30 mM samples.

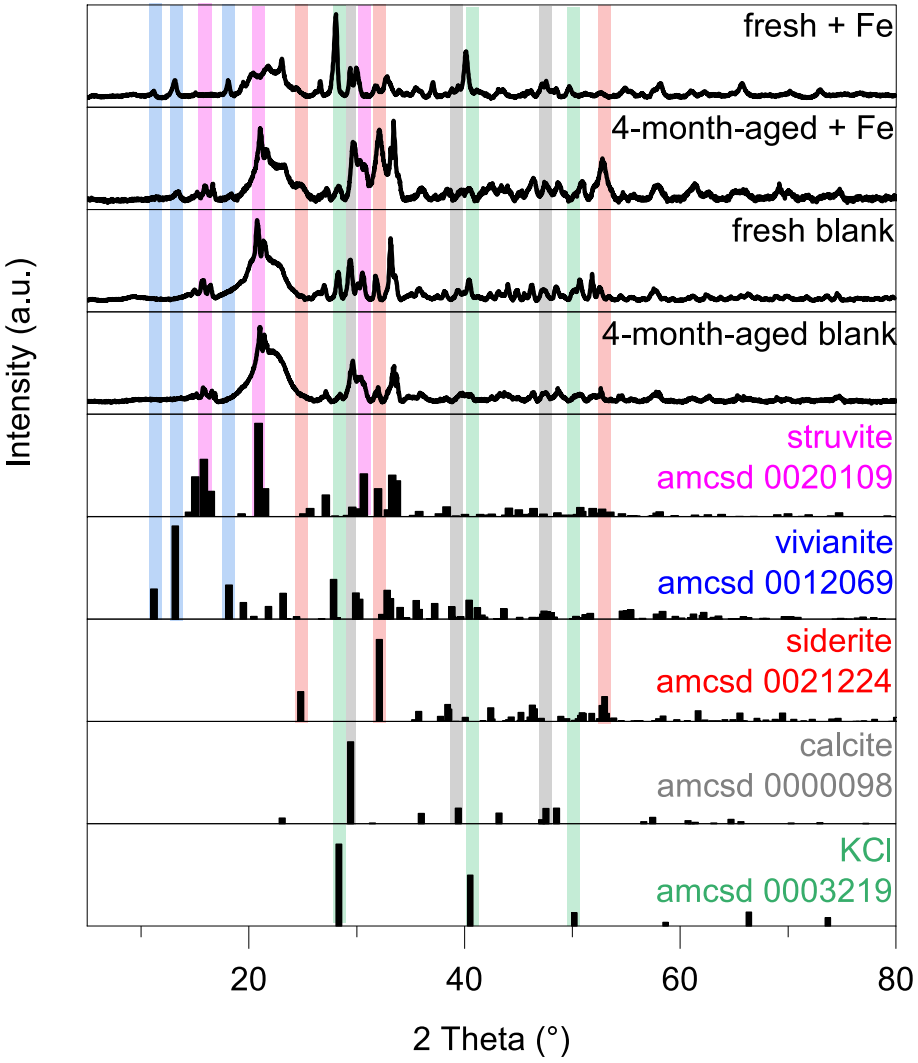

Fig. 2. Baseline corrected XRD patterns of blank and iron amended fresh and 4-month-aged manures with the identified crystal phases [70].

X-ray diffraction analysis (Fig. 5) supported the trends observed in the liquid phase. Siderite reflections were detected at elevated DIC, confirming that both carbonate and phosphate were competing for iron under these conditions. However, at low DIC concentrations, vivianite reflections were relatively weak, while higher DIC concentrations corresponded with diminished struvite. At the highest DIC levels, a broad hump in the XRD patterns between 15° and 25° 2θ suggested the formation of an amorphous or nanoparticulate phase which could be related to the precipitation of fine iron minerals or the dissolution of struvite to small particles.

Despite the qualitative similarities, notable discrepancies exist between the ultrapure water system and the manure matrix. One key difference was, as mentioned in 3.2, that struvite and iron were less concentrated than in manure. Moreover, the higher ionic strength in manure will influence the solubility of the ions and crystallization in the system. Generally, an increased ionic strength decreases the activity coefficient of ions and their likelihood to precipitate. However, if more ions of the same type are present, they are more likely to precipitate [53]. In fresh manure, more vivianite precipitation than in the ultrapure system was observed, which could be due to the higher concentration of iron that was added to the solution. Nevertheless, assessing the effect of ionic strength is more complicated due to the diverse composition of ions in manure.

Another notable difference between the ultrapure system and the manure system is the counter ion of carbonate. Sodium bicarbonate was used in the ultrapure system, whereas DIC is known to balance out ammonium in manure matrices [54]. Given that struvite solubility is sensitive to the concentrations of its constituent ions—magnesium, phosphate, and ammonium—the high ammonium levels in manure (Table 1) are likely to suppress struvite dissolution at higher DIC. Modeling the experimental conditions in ultrapure water at pH 8 using MINTEQ confirmed that increasing ammonium concentrations theoretically reduce the extent of struvite dissolution, as indicated by dissolved magnesium (Fig. A 4). In the absence of ammonium, struvite dissolution could be increased in the presence of DIC due to the formation of dissolved magnesium carbonate and bicarbonate complexes. MINTEQ predicted all magnesium to be dissolved at 300 mM DIC using sodium as a counter ion, with 36 % present as magnesium bicarbonate and 10 % present as magnesium carbonate. Hence, the choice of the carbonate counter ion plays an important role in reproducing the manure system in ultrapure water. However, in the case of fresh manure, ammonium concentrations are similarly elevated as those in 4-month-aged manure (390 mM and 400 mM, respectively). Therefore, the high DIC seems to play a more significant role in preventing vivianite formation from struvite than high ammonium concentrations in solution.

3.3. DIC stripping of digested manure

Since a high DIC seems to be the main reason for the absence of vivianite formation in manure systems, working with fresh manure

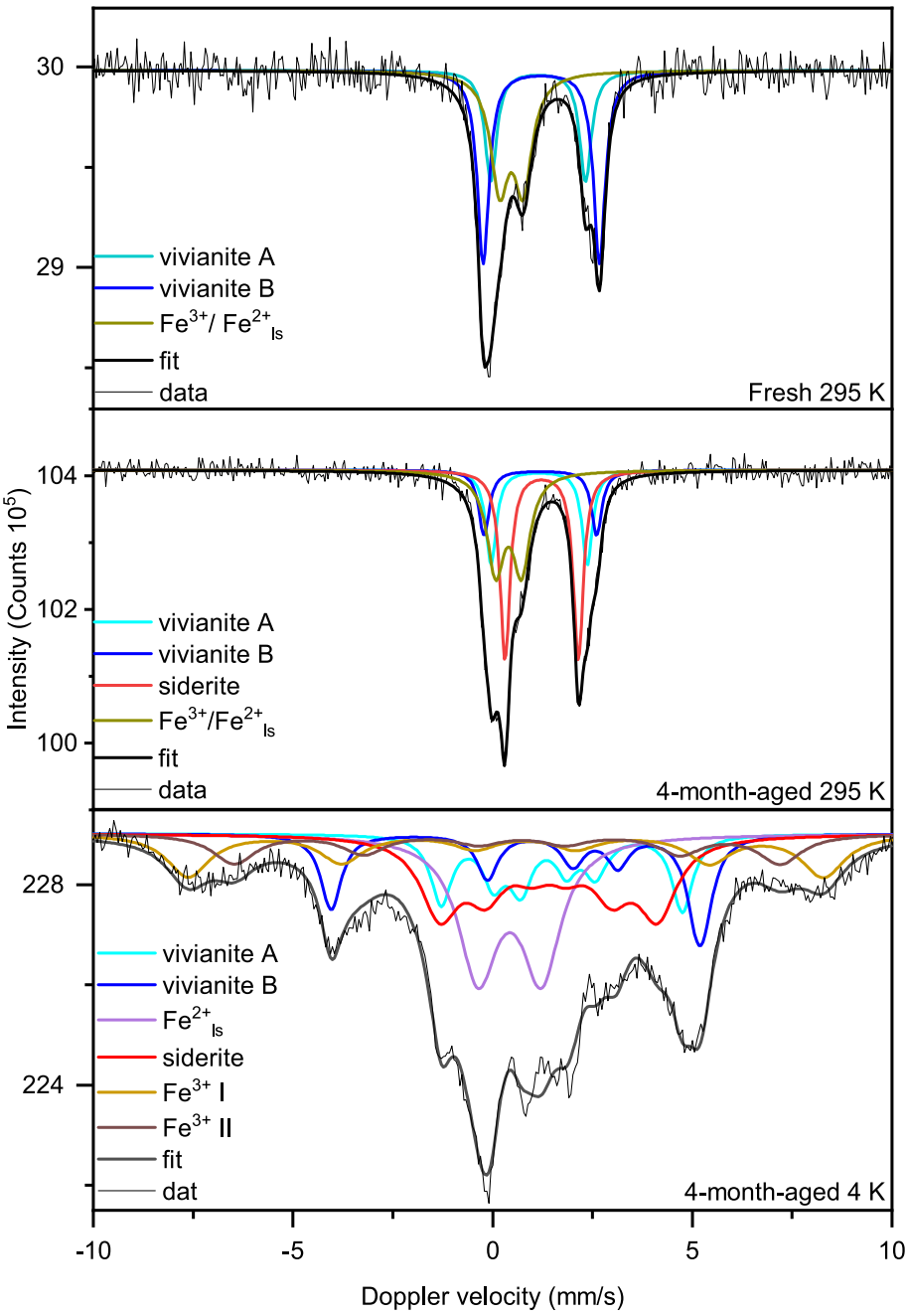

Fig. 3. Mössbauer spectra at 295 K of fresh manure and at 295 K and 4 K of 4-month-aged manure with fitted iron phases.

could be recommended. An alternative could be progressively removing DIC from aged or digested manure, which can even be combined with ammonia stripping of digested manure, reducing both DIC and ammonium in the manure (Section 2.2). Fig. 6 presents Mössbauer spectra of the solids of five iron dosed digested manure samples subjected to ammonia stripping, hence with different DIC levels. Relevant Mössbauer parameters are summarized in Table 5. Consistent with previous observations in fresh and 4-month-aged manure, iron speciation in digested manure was dominated by phosphate-, sulfide-, or carbonate-bound forms. In the sample with the highest DIC concentration, siderite and iron(III)/low-spin iron(II) species— which could be attributed to iron sulfides similarly to what was done in Section 3.1—were the only identified iron-containing phases. As DIC concentrations decreased, the relative spectral contribution of vivianite increased, accompanied by a decline in the siderite and iron(III)/low-spin iron(II) phases' abundance. However, the proportion of the iron(III)/low-spin iron(II) sulfide phase in the less stripped digested manure samples appears disproportionately high when compared to the sulfur content in manure, assuming the maximum Fe/S molar ratio of 1 (see Section 3.1). This discrepancy suggests that part of this spectral contribution may arise from unidentified iron(III) and/or low-spin iron(II) phases distinct from iron sulfides (see Table 5). In fact, the elevated line width of these contributions also supports a small particle size, which could stem from small iron(III) particles such as ferrihydrite. Table 6 illustrates that decreasing DIC concentrations correlate with a lower contribution from these unattributed iron phases. Due to the limitation of having Mössbauer spectra only from measurements performed at 295 K, further identification of these phases remains speculative. At this temperature, the phase is consistent with either a low-spin iron(II) or an iron(III) species. However, low-spin iron(II) phases other than iron sulfides are unlikely to

Table 4
Distribution of Fe species according to Mössbauer analysis at 295 K measurements of fresh manure and 295 K and 4 K measurements of 4-month-aged manure, with isomer shift (IS), quadrupole splitting (QS), magnetic field (B), line width (LW), and related Fe spectral contribution percentage (% Fe). The last column shows the estimated percentage of P in vivianite based on vivianite quantification from Mössbauer analysis. Errors: IS, QS, LW ± 0.01 mm/s; B ± 1 T; % Fe ± 3 %.

	T	Fe species	*IS* (mm/s)	*QS* (mm/s)	*B* (T)	*LW* (mm/s)	% Fe	% P in vivianite
Fresh manure	295 K	vivianite A	1.14	2.37	–	0.35[a]	23	97
		vivianite B	1.22	2.91	–	0.35[a]	41	
		Fe(III)/ ls Fe (II)	0.47	0.59	–	0.55	36	
4-month-aged manure	295 K	vivianite A	1.16	2.41	–	0.32[a]	19	49
		vivianite B	1.19	2.81	–	0.32[a]	13	
		siderite	1.23	1.85	–	0.31	37	
		Fe(III)/ ls Fe (II)	0.38	0.68	–	0.51	31	
4-month-aged manure	4 K	vivianite A	1.56	1.86	28	0.62[a]	13	41
		vivianite B	1.51	2.21	16	0.62[a]	14	
		Fe(III) vivianite A	0.54	−0.36	43	1.30[a]	9	
		Fe(III) vivianite B	0.57^	−0.49	49	1.30[a]	15	
		low spin Fe (II)	0.43	1.58	–	1.19[b]	26	
		siderite	1.43	–	17	1.16[b]	26	

[a] Fixed same line width for vivianite A and B contributions.
[b] Fixed parameters.

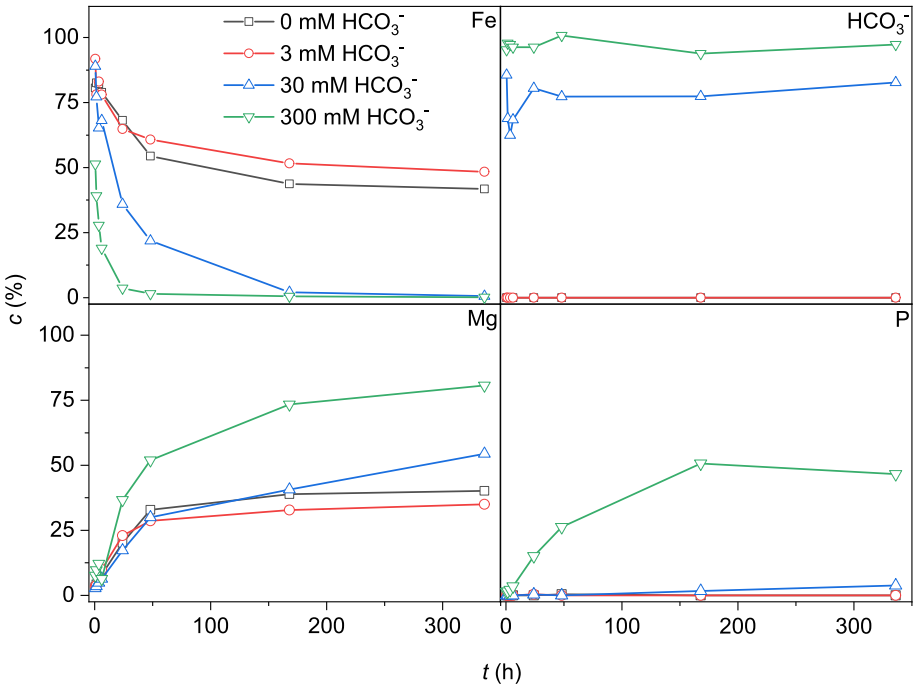

Fig. 4. Time-dependent concentrations of dissolved species in ultrapure water at varied $NaHCO_3$ concentrations, with 5 mM struvite, 7.5 mM $FeCl_2$, and pH 8.

form in manure, as such species typically require strong-field ligands like cyanide, carbonyl, or synthetic chelators (e.g., bipyridine) [55], which are not typically found in manure matrices [54]. Consequently, the presence of iron(III) species appears more plausible, suggesting oxidation of the siderite phase.

Siderite oxidizes easily [56,57] and it is conceivable that partial oxidation occurred during sample preparation. Rothwell et al. (2025) demonstrated that synthetic siderite oxidizes within hours under ambient conditions, although partial Fe(II) preservation was observed for up to 500 h in the presence of low-molecular-weight organic acids, compounds also found in manure [58]. These acids could therefore account for the coexistence of the preserved siderite together with the oxidized iron(III) phases, while vivianite oxidized more slowly. Alternatively, kinetic constraints may have influenced phase development. Like in fresh manure, magnesium went into solution upon iron addition to the digested manure samples, indicating the dissolution of struvite. Equilibrium was assumed to be reached after 48 h based on the stabilization of dissolved magnesium concentrations, indicative of struvite dissolution (see Figs. A 3, A 5, A 6). Unlike magnesium, no dissolved phosphate was detected post-treatment, suggesting that phosphate was incorporated into another solid phase, presumably vivianite. Notably, in a separate proof-of-concept experiment, Prot et al. conducted Mössbauer spectroscopy on samples of manure dosed with 11 g/L iron after one day and five weeks [20]. They observed a significant reduction in the iron (III)/low-spin iron(II) spectral contribution—from 63 % to 27 %, respectively — concurrent with increased vivianite and siderite signals. This finding suggests that additional vivianite and siderite may have formed in high-DIC samples when the experiments had been conducted over longer timeframes.

While vivianite formation correlates with lowering the DIC, struvite dissolution could also be related to lowering the ammonium concentration, as elaborated in Section 3.2. In this set of experiments, both DIC and ammonium concentrations were lowered through stripping. In comparison to magnesium dissolution in fresh manure, the magnesium dissolution happened faster in the stripped digested samples. The magnesium release seemed to stabilize after 24 h in the former, while it was

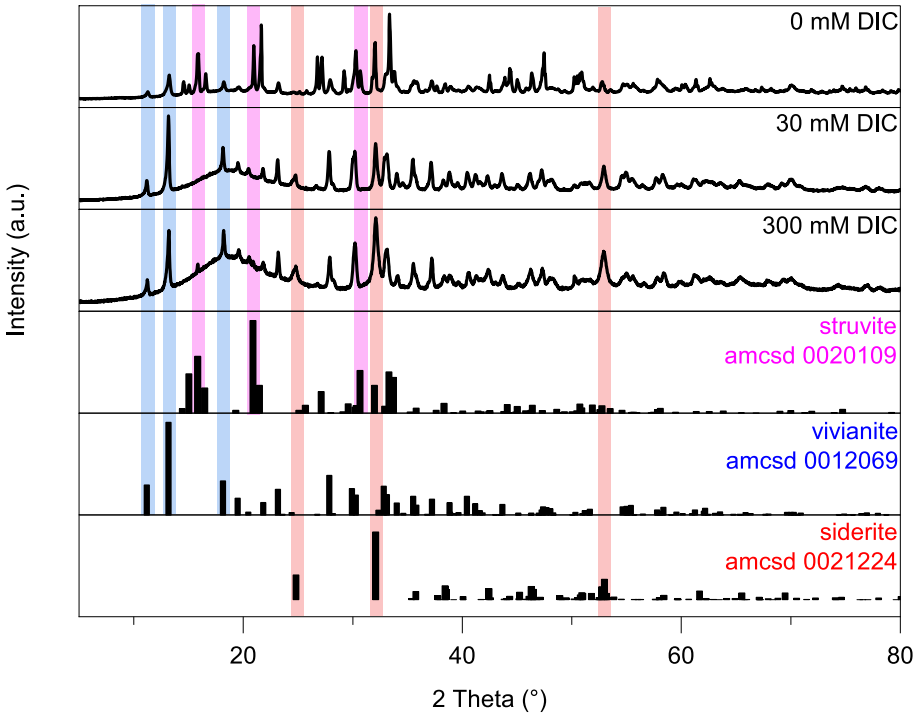

Fig. 5. Baseline corrected XRD patterns of the precipitates in the vivianite vs siderite formation experiment in ultrapure water with varied $NaHCO_3$ concentrations, 5 mM struvite, 7.5 mM $FeCl_2$, and at pH 8, together with the identified crystal phases [70].

after 4 h in the latter. As was discussed by Schott et al. [27,28], and in Section 3.2, DIC is the main barrier in the formation of calcium and iron phosphates, respectively. However, lowered ammonium concentrations influence the kinetics of struvite dissolution, and this could have a further influence on the formation of the iron phosphate phase. To fully elucidate the transformation pathways of iron species in manure, further time-resolved solid-phase characterization in the initial hours following iron addition is necessary.

3.4. DIC thresholds for vivianite formation in digested manure, THP digested sludge, and raw manure

As discussed in Section 3.3, a reduction in dissolved inorganic carbon (DIC) in digested manure significantly promotes the formation of vivianite. Mössbauer spectroscopy enabled quantification of iron incorporated into vivianite, allowing for correlation with the DIC concentration of each sample. To facilitate a more accurate comparison, the estimated amount of iron present as iron sulfide—assuming a stoichiometric Fe/S ratio of 1—was subtracted from the total iron content. This correction yielded the percentage of iron attributed to vivianite, adjusted for sulfur interference, as outlined in Section 3.1. The molar amount of iron in vivianite was calculated using Eq. (4):

$$\text{Fe in vivianite} = (\%\ \text{Fe vivianite A} + \%\ \text{Fe vivianite B}) \bullet \text{total Fe} \quad (4)$$

The sulfur-corrected percentage of iron in vivianite was then determined using Eq. (5):

$$\%\ \text{Fe in vivianite corrected for S} = \frac{\text{Fe in vivianite}}{\text{total Fe} - \text{total S}} \bullet 100\% \quad (5)$$

With % Fe vivianite A and B as determined by Mössbauer spectroscopy, total Fe and S, the total molar concentration of the element determined at the end of the experiment.

Fig. 7a illustrates the inverse relationship between DIC concentration and sulfur-corrected % Fe in vivianite. The data exhibits a slightly sigmoidal trend, with vivianite formation approaching a maximum at approximately 55 mM DIC. A more pronounced increase in vivianite content is observed below 30 mM DIC, suggesting a threshold for optimal vivianite formation between 30 and 55 mM DIC. This corresponds to a bicarbonate concentration of approximately 2–3 g/L. This threshold aligns with typical bicarbonate concentrations in digested sludge, which are around 3 g/L [59], supporting the hypothesis that vivianite formation in sludge is generally limited by sulfide availability rather than DIC [35,37,60]. However, minor siderite formation has been reported in Finnish sludge samples, potentially due to elevated iron concentrations [17]. Prot et al. also reported higher DIC concentrations in sludge—up to 6.3 g/L HCO_3^- (approximately 100 mM DIC)—which, based on the present findings, may inhibit vivianite formation. Such elevated DIC levels are particularly relevant in thermal hydrolysis plants (THPs), where ammonium concentrations can reach approximately 120 mM due to enhanced protein degradation [61,62]. This increase in ammonium is typically balanced by a corresponding rise in DIC. Indeed, THP-derived digested sludge samples (Table A 2) exhibited both elevated DIC and siderite formation, along with reduced vivianite content as detected with Mössbauer spectroscopy (Fig. A 7, Table A 3). Notably, the vivianite content at these DIC levels aligns with the trend observed in stripped digested manure (blue triangle in Fig. 7a), suggesting that the findings from digested manure can be extrapolated to wastewater treatment systems with elevated DIC, such as THPs.

Whether the observed relationship between DIC concentration and iron incorporation into vivianite also applies to fresh and 4-month-aged manure remains to be fully established. Additionally, the extent to which this relationship can be predicted using the MINTEQ software for chemical equilibrium modeling was explored (Table 2 and Table A 2). Notably, both fresh and 4-month-aged manure exhibited elevated phosphate concentrations, attributed to higher total solids (TS) content (see Table 1), which necessitated proportionally higher iron dosing to achieve comparable vivianite formation. To enable consistent comparison across samples with varying DIC and competing anion concentrations, the absolute DIC values from Fig. 7a were normalized. This was achieved by dividing the combined molar concentrations of phosphate and sulfide by the DIC concentration of each sample. A stoichiometric Fe/S molar ratio of 1 was assumed (as discussed in Section 3.1), while

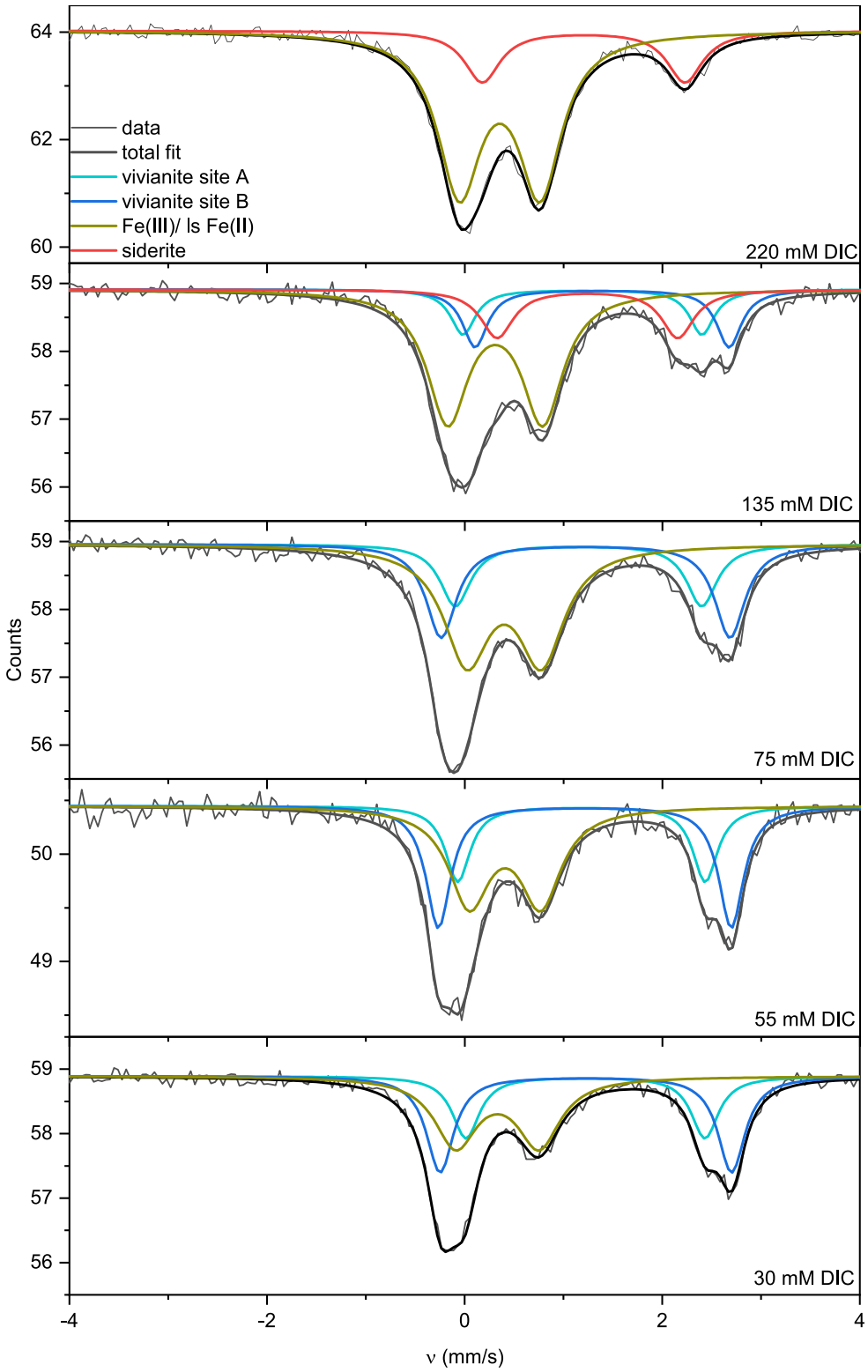

Fig. 6. Mössbauer spectra at 295 K of stripped digestated manure with different DIC content, with fitted iron phases.

for phosphate, the stoichiometric Fe/P ratio of 1.5—corresponding to vivianite—was applied. This yielded the dimensionless parameter:

$$(1.5\,P + S)/DIC$$

Fig. 7b presents a comparison of this normalized parameter across stripped digested manure, fresh and 4-month-aged manure, and THP-derived digested sludge (represented by squares, dots, diamonds, and triangles, respectively). Experimental data are contrasted with MINTEQ predictions, with filled symbols representing measured values and outlined symbols representing model outputs. Experimentally, vivianite formation plateaued at a normalized ratio of approximately 2–3 in both fresh and stripped digested manure. Interestingly, 4-month-aged manure supported more efficient vivianite formation at lower normalized ratios. However, quantification of vivianite in the 4-month-aged

Table 5
Distribution of Fe species according to Mössbauer analysis at 295 K of stripped digested manure with different DIC content, with isomer shift (IS), quadrupole splitting (QS), line width (LW), and related Fe spectral contribution percentage (% Fe). The last column shows the estimated percentage of P in vivianite based on vivianite quantification from Mössbauer analysis. Error IS, QS, LW ± 0.01 mm/s; % Fe ± 3 %.

	Fe species	IS (mm/s)	QS (mm/s)	LW	% Fe	% P in vivianite
220 mM DIC	Siderite	1.2	2.05	0.44	21	
	Fe(III)/ ls Fe (II)	0.35	0.82	0.53	79	
	Vivianite A	1.23	2.36	0.29[a]	11	
	Vivianite B	1.20	2.94	0.29[a]	15	
135 mM DIC	Siderite	1.23	1.89	0.42	19	36
	Fe(III)/ ls Fe (II)	0.37	0.84	0.52	57	
	Vivianite A	1.23	2.44	0.34[a]	17	
	Vivianite B	1.24	2.93	0.34[a]	25	
75 mM DIC	Siderite	1.28	1.91	0.45	7	53
	Fe(III)/ls Fe (II)	0.34	0.86	0.55	52	
	Vivianite A	1.18	2.5	0.30[a]	21	
	Vivianite B	1.22	2.96	0.30[a]	34	65
55 mM DIC	Fe(III)/ ls Fe (II)	0.41	0.72	0.5	44	
	Vivianite A	1.22	2.41	0.33[a]	23	
	Vivianite B	1.23	2.96	0.33[a]	36	67
30 mM DIC	Fe(III)/ ls Fe (II)	0.33	0.85	0.52	41	

[a] Fixed same line width for vivianite A and B contributions.

Table 6
Mössbauer spectral contributions of total iron(III)/ low spin iron (II) at different DIC concentrations (from Table 5), and their estimated fractionations in maximum FeS phase content (based on total sulfur in the manure sample), and unattributed Fe phases (other than FeS) content.

Sample	Iron(III)/low spin iron(II)	Max. FeS (%)	Unattributed Fe (%)
220 mM DIC	79	34	45
135 mM DIC	57	33	24
75 mM DIC	52	37	14
55 mM DIC	44	40	5
30 mM DIC	40	41	–

manure sample via Mössbauer spectroscopy proved more challenging, likely due to sample-specific complexities such as mineral inhomogeneity or particle size effects. In contrast, for the other manure samples, the extent of struvite dissolution—assessed via magnesium and ammonium release—correlated well with phosphate incorporation into vivianite as determined by Mössbauer analysis (Fig. A 6), supporting the reliability of the method in those cases. In the 4-month-aged manure sample, however, the observed struvite dissolution was lower than expected based on Mössbauer-derived vivianite content. This discrepancy suggests a potential overestimation of vivianite by Mössbauer spectroscopy in this specific case, possibly due to the aforementioned factors.

Geochemical modeling using MINTEQ was employed to assess the thermodynamic predictability of DIC as a barrier to vivianite formation. The MINTEQ simulations predicted a sharp increase in vivianite formation—from 0 % to 90 %—at normalized DIC ratios below 1. In contrast, experimental data revealed a more gradual increase in vivianite formation, especially in stripped digested manure samples with intermediate DIC concentrations (75–135 mM) and in thermal hydrolysis process (THP) sludge (140 mM DIC). These discrepancies could be attributed to shortcomings of the thermodynamic model and kinetic factors influencing phase transformations in real complex matrices. To improve the thermodynamic predictions, the model could be extended by incorporating more accurate solubility constants for impure mineral phases, for example. Moreover, the limitations of the model are particularly pronounced under high ionic strength conditions, where solubility and equilibrium behavior become increasingly complex. Ionic strength values calculated by MINTEQ ranged from 0.3 M (30 mM DIC digested manure) to 0.6 M (4-month-aged manure). As noted by Hafner and Bisogni (2009), modeling solubility and pH-dependent equilibria in matrices rich in ammonia and carbonate presents significant challenges [63]. Although the Specific Ion Interaction Theory (SIT) implemented in MINTEQ provides ionic activity corrections, it may still fall short in accurately capturing solubility dynamics in manure systems. Shorter retention times also play a role in real matrices, potentially favoring the precipitation of one phase over another kinetically. This has been observed in calcium phosphate formation in solid waste streams [64]. It is important to recognize the relevance of kinetic limitations in wastewater and manure treatment systems, since they operate on shorter, standardized timescales, unlike geochemical processes in soils. Ultimately, while MINTEQ simulations were instrumental in identifying siderite formation as a potential barrier to vivianite precipitation at elevated DIC levels, the model—originally developed for geological systems—lacks the resolution to predict phase speciation near threshold

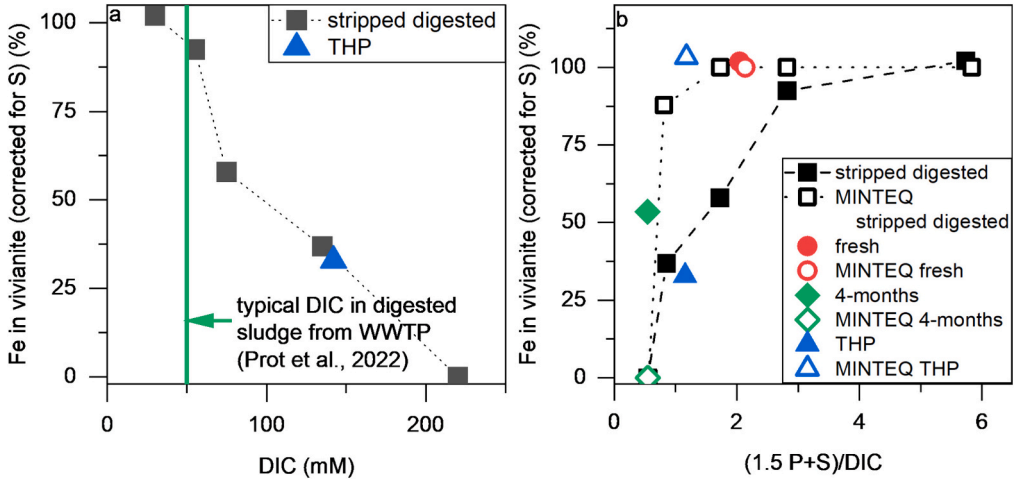

Fig. 7. a. Relative amount of iron in vivianite corrected for the sulfur content at different DIC concentrations in stripped digested manure and THP samples. b Relative amount of iron in vivianite corrected for the sulfur content (assumed Fe/S molar ratio of 1), against the (1.5 P*1.5 + S)/DIC molar ratio, in the stripped digested manure, fresh manure, 4-month-aged manure, and THP samples. For all cases, both experimental data (full symbols) and simulated data from MINTEQ (outlined symbols) are represented.

values in complex waste matrices, which could lead to underestimation of the role of siderite around these values. Further research is needed to develop these models and understand kinetic limitations in complex waste matrices and their treatment processes.

Overall, a normalized ratio of approximately 2.5 appears to serve as a practical threshold for maximizing vivianite formation in both raw and digested manure. The required molar iron concentration for vivianite formation can be estimated using Eq. (6):

$$\mathrm{Fe} = (1.5\ \mathrm{total\ P} + \mathrm{total\ S}) \bullet 2.5\ \mathrm{DIC} \quad (6)$$

Above this threshold, vivianite formation increases only marginally, indicating a plateau effect. Below this ratio, vivianite yields decline sharply, particularly in digested manure, where competing iron carbonate phases such as siderite may form and sequester iron, thereby reducing the efficiency of vivianite precipitation.

3.5. Outlook on vivianite formation in systems high in DIC

In pig farming in the Netherlands, livestock densities are high with limited land to manure production, leading to a surplus of nutrients and removing P and other nutrients in a targeted way would be beneficial for their redistribution [10]. The limitation of dissolved inorganic carbon (DIC) as a limiting factor for vivianite formation in pig manure introduces a new possibility for phosphate recovery through iron dosing strategies. One potential approach involves promoting vivianite crystallization directly within the fresh manure, a process demonstrated to be feasible in this study (97 % of the phosphorus bound as vivianite). Nevertheless, this method presents notable challenges. The high solids content in fresh manure complicates magnetic separation, but the implementation of such a phosphate recovery system would require substantial adjustments to current manure management practices to avoid storage, a condition not always operationally feasible.

An alternative strategy involves utilizing digested pig manure, with the known benefits from anaerobic digestion processes that not only stabilize organic matter but also generate biogas [34], thus enhancing overall resource circularity. Integrating vivianite recovery into manure digestion could enable the simultaneous extraction of multiple resources: energy via biogas, ammonia through stripping (potentially coupled with carbon capture), and phosphate. However, based on the characteristics of the digested manure used in this study, approximately 90 % of the dissolved DIC would need to be removed to achieve a bicarbonate concentration of 3 g/L—necessary for efficient vivianite formation. Some facilities already couple ammonia stripping of manure or food waste to CO_2 stripping to keep the pH high enough, reducing the addition of base [71]. Such processes could be adapted to reach a lower DIC suitable for vivianite formation. However, practical application substituting nitrogen gas with other stripping gases such as air and methane, or vacuum stripping [65] should be tested, since using pure nitrogen gas is too expensive. Moreover, vivianite particles in digested manure were smaller than those found in digested sludge (Fig. A 8). Their magnetic separation from digested manure has yet to be demonstrated at a larger scale. Hence, further testing is necessary to perform an economic analysis of this process. Ultimately, the viability of this technology will depend on market demand for refined vivianite-based products and the availability of sustainable electricity for energy-intensive pumping processes [66].

Overall, the limitation of vivianite formation at elevated DIC concentrations provides new insights into the geochemical conditions favoring vivianite precipitation. DIC levels in most lake sediments or wastewater sludges are generally lower, thereby exerting a less significant influence. However, the high DIC in certain wastewater treatment contexts, such as THP digested sludge, poses a barrier to vivianite formation in line with the observations in digested manure in these plants. Interestingly, Wang et al. observed higher vivianite formation (based on XANES quantification) in hydrothermally digested samples compared to conventionally digested sludge [67]. In contrast, Wang et al. identified barriers to vivianite formation in hydrothermally treated digested sludge, attributing these to magnesium availability and pH [68], while Cui et al. (2024) pointed to iron-organic complexation as the limiting factor [69]. Notably, none of these studies investigated the potential role of DIC. Therefore, the role of siderite formation in iron dosed sludges high in DIC might have been overlooked so far. One reason could be that siderite is not detected due to oxidation prior to the measurements if the samples were not protected accordingly. Further research using techniques such as Mössbauer spectroscopy could help clarify the influence of DIC in vivianite formation in sludge matrices high in DIC.

4. Conclusion

This study demonstrated that elevated DIC concentrations are the main barrier to vivianite formation in both raw and digested manure experiments, as well as THP digested sludge. A stoichiometric iron dose of $\mathrm{Fe} = (1.5\ \mathrm{P} + \mathrm{S}) \bullet 2.5\ \mathrm{DIC}$ was identified as critical for optimal vivianite precipitation. Longer retention times may further enhance yields and merit future investigation. In the absence of ammonium and high ionic strength, vivianite formation from struvite at decreased DIC could not be reproduced in ultrapure water, with thermodynamic modeling indicating ammonium to be a relevant ion in vivianite formation from struvite besides DIC.

While challenging, vivianite recovery from pig manure offers potential for integrated biomethane, nitrogen, and phosphorus recovery as well as carbon capture. A possible approach involves stripping DIC and ammonia from digested manure, followed by iron dosing and magnetic separation of vivianite. However, practical implementation requires further testing with alternative stripping gases and at larger scales to evaluate feasibility.

CRediT authorship contribution statement

Sophie Banke: Writing – original draft, Visualization, Methodology, Investigation, Formal analysis, Data curation, Conceptualization. **Jacobo Meca Romero:** Writing – original draft, Investigation, Formal analysis, Data curation. **Alexandre Monteiro:** Writing – original draft, Visualization, Investigation, Formal analysis, Data curation. **Thomas Prot:** Writing – review & editing, Supervision, Methodology, Conceptualization. **Leon Korving:** Writing – review & editing, Supervision, Methodology, Funding acquisition, Conceptualization. **Carlo Belloni:** Writing – review & editing, Validation, Formal analysis. **Chris Schott:** Writing – review & editing, Validation, Conceptualization. **Iulian A. Dugulan:** Writing – review & editing, Validation, Formal analysis. **Mark C. M.van Loosdrecht:** Writing – review & editing, Supervision, Methodology, Funding acquisition, Conceptualization.

Declaration of Generative AI and AI-assisted Technologies in the Writing Process

During the preparation of this work the author(s) used Chat GPT in order to improve the writing style. After using this tool, the authors reviewed and edited the content as needed and take full responsibility for the content of the published article.

Declaration of competing interest

The authors declare that they have no known competing financial interests or personal relationships that could have appeared to influence the work reported in this paper.

Acknowledgment

This work was performed in the cooperation framework of Wetsus, European Centre of Excellence for Sustainable Water Technology (www.

wetsus.nl). Wetsus is co-funded by the European Union (Horizon Europe, LIFE, Interreg and EDRF), the Province of Fryslân and the Dutch Government: Ministry of Economic Affairs (TTT, SBO & PPS-I/TKI Water Technology), Ministry of Education, Culture and Science (TTT & SBO) and Ministry of Infrastructure and Water Management (National Growth Fund - UPPWATER). This project has received funding from the European Union's Horizon 2020 Research and Innovation Programme under the Marie Skłodowska-Curie grant agreement No 956454 (RecaP). The authors like to thank the participants of the research theme "Phosphate recovery" for the fruitful discussions and their financial support. Ruud Hendrikx at the Department of Materials Science and Engineering of the Delft University of Technology is acknowledged for the X-ray analysis. The authors thank the CCS Energie-advies and pig farm Tijs in Hoge Hexel for the manure, and Waterschap Vechtstromen for the THP digested sludge.

Appendix A. Supplementary data

Supplementary data to this article can be found online at https://doi.org/10.1016/j.cej.2025.169019.

Data availability

Data will be made available on request.

References

[1] G. Tóth, R.-A. Guicharnaud, B. Tóth, T. Hermann, Phosphorus levels in croplands of the European Union with implications for P fertilizer use, Eur. J. Agron. 55 (2014) 42–52, https://doi.org/10.1016/j.eja.2013.12.008.
[2] P. Panagos, J. Köningner, C. Ballabio, L. Liakos, A. Muntwyler, P. Borrelli, E. Lugato, Improving the phosphorus budget of European agricultural soils, Sci. Total Environ. 853 (2022) 158706, https://doi.org/10.1016/j.scitotenv.2022.158706.
[3] R.B. Chowdhury, G.A. Moore, A.J. Weatherley, M. Arora, Key sustainability challenges for the global phosphorus resource, their implications for global food security, and options for mitigation, J. Clean. Prod. 140 (2017) 945–963, https://doi.org/10.1016/j.jclepro.2016.07.012.
[4] D.W. Schindler, S.R. Carpenter, S.C. Chapra, R.E. Hecky, D.M. Orihel, Reducing phosphorus to curb Lake eutrophication is a success, Environ. Sci. Technol. 50 (2016) 8923–8929, https://doi.org/10.1021/acs.est.6b02204.
[5] CBS, Livestock Manure; Production, Transport and Use, Key Figures, 2025 https://www.cbs.nl/en-gb/figures/detail/83981ENG (accessed July 4, 2025).
[6] F.R. Leenstra, T.V. Vellinga, F. Neijenhuis, F.E. de Busonje, Manure: A Valuable Resource., Wageningen UR Livestock Research, 2014, p. 35.
[7] O.F. Schoumans, P.A.I. Ehlert, J.A. Nelemans, W. van Tintelen, W.H. Rulkens, O. Oenema, Explorative Study of Phosphorus Recovery from Pig Slurry, Alterra, 2014.
[8] P.H. Pagliari, C.A.M. Laboski, Investigation of the inorganic and organic phosphorus forms in animal manure, J. Environ. Qual. 41 (2012) 901–910, https://doi.org/10.2134/jeq2011.0451.
[9] J. Wu, X. Zhong, Relationship between the particle size and nutrient distribution of feces and nutrients in pigs and dairy cows and the efficiency of solid-liquid separation, IOP Conf Ser Earth Environ Sci 514 (2020) 052035, https://doi.org/10.1088/1755-1315/514/5/052035.
[10] M. van der Hoek, Dutch Loss of Manure Derogation, 2024.
[11] O.F. Schoumans, F. Bouraoui, C. Kabbe, O. Oenema, K.C. van Dijk, Phosphorus management in Europe in a changing world, Ambio 44 (2015) 180–192, https://doi.org/10.1007/s13280-014-0613-9.
[12] C.-H. Zhou, H.-J. Huang, L. Li, Z.-Q. Pan, X.-F. Xiao, J.-X. Wang, Advances in Hydrothermal Carbonization of Livestock Manure, 2020, pp. 183–205, https://doi.org/10.1007/978-3-030-42284-4_7.
[13] X. Su, T. Zhang, J. Zhao, S. Mukherjee, N.M. Alotaibi, S.F. Abou-Elwafa, H.-T. Tran, N.S. Bolan, Phosphorus fraction in hydrochar from co-hydrothermal carbonization of swine manure and rice straw: an optimization analysis based on response surface methodology, Water (Basel) 16 (2024) 2208, https://doi.org/10.3390/w16152208.
[14] A.A. Szögi, M.B. Vanotti, P.G. Hunt, Phosphorus recovery from pig manure solids prior to land application, J. Environ. Manage. 157 (2015) 1–7, https://doi.org/10.1016/j.jenvman.2015.04.010.
[15] W. Tao, K.P. Fattah, M.P. Huchzermeier, Struvite recovery from anaerobically digested dairy manure: a review of application potential and hindrances, J. Environ. Manage. 169 (2016) 46–57, https://doi.org/10.1016/j.jenvman.2015.12.006.
[16] P. Wilfert, P.S. Kumar, L. Korving, G.-J. Witkamp, M.C.M. van Loosdrecht, The relevance of phosphorus and Iron chemistry to the recovery of phosphorus from wastewater: a review, Environ. Sci. Technol. 49 (2015), https://doi.org/10.1021/acs.est.5b00150.
[17] T. Prot, V.H. Nguyen, P. Wilfert, A.I. Dugulan, K. Goubitz, D.J. De Ridder, L. Korving, P. Rem, A. Bouderbala, G.J. Witkamp, M.C.M. van Loosdrecht, Magnetic separation and characterization of vivianite from digested sewage sludge, Sep. Purif. Technol. 224 (2019), https://doi.org/10.1016/j.seppur.2019.05.057.
[18] W.K. Wijdeveld, T. Prot, G. Sudintas, P. Kuntke, L. Korving, M.C.M. van Loosdrecht, Pilot-scale magnetic recovery of vivianite from digested sewage sludge, Water Res. 212 (2022), https://doi.org/10.1016/j.watres.2022.118131.
[19] C. Li, Y. Sheng, H. Xu, Phosphorus recovery from sludge by pH enhanced anaerobic fermentation and vivianite crystallization, J. Environ. Chem. Eng. 9 (2021) 104663, https://doi.org/10.1016/j.jece.2020.104663.
[20] T. Prot, Phosphorus Recovery From Iron-coagulated Sewage Sludge, 2021, pp. 201–232, https://doi.org/10.4233/uuid:3d31068b-259a-4798-8723-be755cc15d23.
[21] EPA, Ecological Soil Screening Level for Iron, Washington, DC, 2003.
[22] J.O. Nriagu, Stability of vivianite and ion-pair formation in the system Fe3(PO4)2-H3PO4H3PO4-H2o, Geochim. Cosmochim. Acta 36 (1972) 459–470, https://doi.org/10.1016/0016-7037(72)90035-X.
[23] K. Lalonde, A. Mucci, A. Ouellet, Y. Gélinas, Preservation of organic matter in sediments promoted by iron, Nature 483 (2012), https://doi.org/10.1038/nature10855.
[24] A. Kleeberg, C. Herzog, M. Hupfer, Redox sensitivity of iron in phosphorus binding does not impede lake restoration, Water Res. 47 (2013), https://doi.org/10.1016/j.watres.2012.12.014.
[25] S. Banke, J. Cottineau, T. Prot, L. Korving, M.C.M. van Loosdrecht, Different influences of organic ligands on vivianite formation and dissolution, J. Environ. Chem. Eng. 13 (2025) 115139, https://doi.org/10.1016/j.jece.2024.115139.
[26] W. Tao, K.P. Fattah, M.P. Huchzermeier, Struvite recovery from anaerobically digested dairy manure: a review of application potential and hindrances, J. Environ. Manage. 169 (2016) 46–57, https://doi.org/10.1016/j.jenvman.2015.12.006.
[27] C. Schott, J.R. Cunha, R.D. van der Weijden, C. Buisman, Innovation in valorization of cow manure: higher hydrolysis, methane production and increased phosphorus retention using UASB technology, Chem. Eng. J. 454 (2023) 140294, https://doi.org/10.1016/j.cej.2022.140294.
[28] C. Schott, L. Yan, U. Gimbutyte, J.R. Cunha, R.D. van der Weijden, C. Buisman, Enabling efficient phosphorus recovery from cow manure: liberation of phosphorus through acidification and recovery of phosphorus as calcium phosphate granules, Chem. Eng. J. 460 (2023) 141695, https://doi.org/10.1016/j.cej.2023.141695.
[29] Eurostat, Agriculture - Manure Storage Statistics, 2025 https://ec.europa.eu/eurostat/statistics-explained/index.php?title=Agriculture_-_manure_storage_statistics (accessed September 10, 2025).
[30] J. Claessens, D. van Gils, T. Brussée, M. Oosterwoud, A. Vrijhoef, A. Plette, M. Kotte, K. Ouwerkerk, M. Gosseling, J. Roskam, F. Taconis, Agricultural Practices and Water Quality in the Netherlands: Status (2020−2023) and Trends (1992–2023). Results of the Monitoring of the Effects of the EU Nitrates Directive Action Programmes, 2024, 2025.
[31] CCS, Biogas Hoge Hexel: mono-mestvergisting op boerderijschaal, 2025 https://www.ccsenergieadvies.nl/projecten/biogas-hoge-hexel/ (accessed September 10, 2025).
[32] A.J. Ward, P.J. Hobbs, P.J. Holliman, D.L. Jones, Optimisation of the anaerobic digestion of agricultural resources, Bioresour. Technol. 99 (2008) 7928–7940, https://doi.org/10.1016/j.biortech.2008.02.044.
[33] H.P. Vu, L.N. Nguyen, Q. Wang, H.H. Ngo, Q. Liu, X. Zhang, L.D. Nghiem, Hydrogen sulphide management in anaerobic digestion: a critical review on input control, process regulation, and post-treatment, Bioresour. Technol. 346 (2022) 126634, https://doi.org/10.1016/j.biortech.2021.126634.
[34] I.M. Nasir, T.I. Mohd Ghazi, R. Omar, Anaerobic digestion technology in livestock manure treatment for biogas production: a review, Eng. Life Sci. 12 (2012) 258–269, https://doi.org/10.1002/elsc.201100150.
[35] T. Prot, W. Wijdeveld, L.E. Eshun, A.I. Dugulan, K. Goubitz, L. Korving, M.C.M. Van Loosdrecht, Full-scale increased iron dosage to stimulate the formation of vivianite and its recovery from digested sewage sludge, Water Res. 182 (2020), https://doi.org/10.1016/j.watres.2020.115911.
[36] C. Schott, J.R. Cunha, R.D. van der Weijden, C. Buisman, Phosphorus recovery from pig manure: dissolution of struvite and formation of calcium phosphate granules during anaerobic digestion with calcium addition, Chem. Eng. J. 437 (2022) 135406, https://doi.org/10.1016/j.cej.2022.135406.
[37] P. Wilfert, A. Mandalidis, A.I. Dugulan, K. Goubitz, L. Korving, H. Temmink, G. J. Witkamp, M.C.M. Van Loosdrecht, Vivianite as an important iron phosphate precipitate in sewage treatment plants, Water Res. 104 (2016) 449–460, https://doi.org/10.1016/j.watres.2016.08.032.
[38] H. Nguyen, T. Prot, W. Wijdeveld, L. Korving, A.I. Dugulan, E. Brück, A. Haarala, M.C.M. van Loosdrecht, Robust magnetic vivianite recovery from digested sewage sludge: evaluating resilience to sludge dry matter and particle size variations, Water Res. 266 (2024) 122407, https://doi.org/10.1016/j.watres.2024.122407.
[39] E. Kuzmann, Z. Homonnay, S. Nagy, K. Nomura, Mössbauer Spectroscopy, in: Handbook of Nuclear Chemistry, Springer US, Boston, MA, 2011, pp. 1379–1446, https://doi.org/10.1007/978-1-4419-0720-2_25.
[40] Z. Klencsár, E. Kuzmann, A. Vértes, User-friendly software for Mössbauer spectrum analysis, J. Radioanal. Nucl. Chem. Artic. 210 (1996) 105–118, https://doi.org/10.1007/BF02055410.
[41] I. Grenthe, A. Plyasunov, K. Spahiu, Estimations of medium effects on thermodynamic data, in: OECD Nuclear Energy Agency (Ed.), Modelling in Aquatic Chemistry, 1997, pp. 325–426.

[42] T. Komiyama, T. Ito, The characteristics of phosphorus in animal manure composts, Soil Sci. Plant Nutr. 65 (2019) 281–288, https://doi.org/10.1080/00380768.2019.1615384.
[43] M. Grodzicki, G. Amthauer, Electronic and magnetic structure of vivianite: cluster molecular orbital calculations, Phys. Chem. Miner. 27 (2000) 694–702, https://doi.org/10.1007/s002690000125.
[44] D. Rouzies, J.M.M. Millet, Mössbauer study of synthetic oxidized vivianite at room temperature, Hyperfine Interact. 77 (1993) 19–28, https://doi.org/10.1007/BF02320295.
[45] J.A. Morice, L.V.C. Rees, D.T. Rickard, Mössbauer studies of iron sulphides, J. Inorg. Nucl. Chem. 31 (1969) 3797–3802, https://doi.org/10.1016/0022-1902(69)80299-X.
[46] C.F. Garibello, A.N. Simonov, D.S. Eldridge, F. Malherbe, R.K. Hocking, Cover feature: redox properties of Iron sulfides: direct *versus* catalytic reduction and implications for catalyst design (ChemCatChem 12/2022), ChemCatChem 14 (2022), https://doi.org/10.1002/cctc.202200617.
[47] L.J. Kubeneck, L.K. ThomasArrigo, K.A. Rothwell, R. Kaegi, R. Kretzschmar, Competitive incorporation of Mn and Mg in vivianite at varying salinity and effects on crystal structure and morphology, Geochim. Cosmochim. Acta 346 (2023), https://doi.org/10.1016/j.gca.2023.01.029.
[48] P. Wilfert, A.I. Dugulan, K. Goubitz, L. Korving, G.J. Witkamp, M.C.M. Van Loosdrecht, Vivianite as the main phosphate mineral in digested sewage sludge and its role for phosphate recovery, Water Res. 144 (2018), https://doi.org/10.1016/j.watres.2018.07.020.
[49] R.E. Vandenberghe, E. De Grave, Application of mössbauer spectroscopy in earth sciences, in: Mössbauer Spectroscopy, Springer Berlin Heidelberg, Berlin, Heidelberg, 2013, pp. 91–185, https://doi.org/10.1007/978-3-642-32220-4_3.
[50] X. Chen, M. Zheng, X. Cheng, C. Wang, K. Xu, Impact of impurities on vivianite crystallization for phosphate recovery from process water of hydrothermal carbonization of kitchen waste, Resour. Conserv. Recycl. 185 (2022) 106438, https://doi.org/10.1016/j.resconrec.2022.106438.
[51] D. Postma, Formation of siderite and vivianite and the pore-water composition of a recent bog sediment in Denmark, Chem. Geol. 31 (1980) 225–244, https://doi.org/10.1016/0009-2541(80)90088-1.
[52] M.P. Huchzermeier, W. Tao, Overcoming challenges to struvite recovery from anaerobically digested dairy manure, Water Environ. Res. 84 (2012) 34–41, https://doi.org/10.2175/106143011X13183708018887.
[53] C.E. Boyd, Solubility and chemical equilibrium, in: Water Quality - An Introduction, 3rd ed., Springer Nature Switzerland AG, Cham, 2020, pp. 65–82.
[54] S.G. Sommer, S. Husted, The chemical buffer system in raw and digested animal slurry, J. Agric. Sci. 124 (1995) 45–53, https://doi.org/10.1017/S0021859600071239.
[55] N. Wiberg, A.F. Holleman, Anorganische Chemie, 103rd ed., De Gruyter, Berlin, 2016.
[56] M. Rothe, A. Kleeberg, M. Hupfer, The occurrence, identification and environmental relevance of vivianite in waterlogged soils and aquatic sediments, Earth Sci. Rev. 158 (2016), https://doi.org/10.1016/j.earscirev.2016.04.008.
[57] W.T. Schaller, A.C. Vlisidis, Spontaneous oxidation of a sample of powdered siderite, Am. Mineral. 44 (1959) 433–435.
[58] K.A. Rothwell, L.K. ThomasArrigo, R. Kaegi, R. Kretzschmar, Low molecular weight organic acids stabilise siderite against oxidation and influence the composition of iron (oxyhydr)oxide oxidation products, Environ Sci Process Impacts 27 (2025) 133–145, https://doi.org/10.1039/D4EM00363B.
[59] T. Prot, L. Korving, M.C.M. Van Loosdrecht, Ionic strength of the liquid phase of different sludge streams in a wastewater treatment plant, Water Sci. Technol. 85 (2022) 1920–1935, https://doi.org/10.2166/wst.2022.057.
[60] L. Heinrich, M. Rothe, B. Braun, M. Hupfer, Transformation of redox-sensitive to redox-stable iron-bound phosphorus in anoxic lake sediments under laboratory conditions, Water Res. 189 (2021), https://doi.org/10.1016/j.watres.2020.116609.
[61] W.P.F. Barber, Thermal hydrolysis for sewage treatment: a critical review, Water Res. 104 (2016) 53–71, https://doi.org/10.1016/j.watres.2016.07.069.
[62] WAVES, WAVES, 2025 https://waves.databank.nl/ (accessed May 26, 2025).
[63] S.D. Hafner, J.J. Bisogni, Modeling of ammonia speciation in anaerobic digesters, Water Res. 43 (2009) 4105–4114, https://doi.org/10.1016/j.watres.2009.05.044.
[64] S. Arabi, A. Umble, S. Trujillo, J. Gage, R. Luna, C. Sigmon, C. Marks, T. Worley-Morse, Phosphorus Sequestration and Recovery with Brushite: Validating Chemical Equilibrium and Process Models with Case Studies, in: WEFTEC 2024, 2024.
[65] M.A. Abdelrahman, A. Khadir, D. Santoro, E. Jang, A. Al-Omari, C. Muller, K. Y. Bell, J. Walton, D. Batstone, G. Nakhla, Vacuum evaporation coupled with anaerobic digestion for process intensification and ammonia recovery: model development, validation and scenario analysis, Bioresour. Technol. 416 (2025) 131753, https://doi.org/10.1016/j.biortech.2024.131753.
[66] J. De Vrieze, G. Colica, C. Pintucci, J. Sarli, C. Pedizzi, G. Willeghems, A. Bral, S. Varga, D. Prat, L. Peng, M. Spiller, J. Buysse, J. Colsen, O. Benito, M. Carballa, S. E. Vlaeminck, Resource recovery from pig manure via an integrated approach: a technical and economic assessment for full-scale applications, Bioresour. Technol. 272 (2019) 582–593, https://doi.org/10.1016/j.biortech.2018.10.024.
[67] F. Wang, S. Ma, X. Han, S. Liu, K. Sun, Enhancing phosphorus release from sewage sludge in anaerobic digestion via thermal hydrolysis pretreatment: insights from phosphorus speciation and molecular biological pathways, Environ. Sci. Technol. 58 (2024) 10828–10838, https://doi.org/10.1021/acs.est.4c01287.
[68] Q. Wang, X. Liu, H. Jung, S. Zhao, S.G. Pavlostathis, Y. Tang, Effect of prestage hydrothermal treatment on the formation of struvite vs vivianite during semicontinuous anaerobic digestion of sewage sludge, ACS Sustain. Chem. Eng. 9 (2021) 9093–9105, https://doi.org/10.1021/acssuschemeng.1c02638.
[69] H. Cui, X. Yang, X. Gao, D. Sun, X. Cheng, Compatibility of vivianite-crystallization pathway of phosphorus recovery with anaerobic digestion systems of thermally hydrolyzed sludge, Environ. Res. 260 (2024) 119640, https://doi.org/10.1016/j.envres.2024.119640.
[70] R.T. Downs, M. Hall-Wallace, The American mineralogist crystal structure database, Am. Mineral. 88 (2003) 247–250, http://rruff.geo.arizona.edu/ (accessed July 4, 2025).
[71] https://www.byosis.com/, 2025 last visited 2025-10-11.
[72] S. Shaddel, T. Grini, S. Ucar, K. Azrague, J.P. Andreassen, S.W. Østerhus, Struvite crystallization by using raw seawater: Improving economics and environmental footprint while maintaining phosphorus recovery and product quality, Water Res. 173 (2020) 115572.